17th World Conference on Earthquake Engineering, 17WCEE
Sendai, Japan - September 13th to 18th 2020

PRELIMINARY STUDY ON DEVELOPMENT OF LIDAR POINT CLOUD DATASET FOR EARTHQUAKE DAMAGE MAPPING BY 3D MACHINE LEARNING

H. Haoyi[(1)], M. Matsuoka[(2)], M. Inoguchi[(3)], K. Kawabe[(4)], K. Horie[(5)]

[(1)] *Graduate Student, Department of Architecture and Building Engineering, Tokyo Institute of Technology, Yokohama 226-8502, Japan; xiu.h.aa@m.titech.ac.jp*
[(2)] *Professor, Department of Architecture and Building Engineering, Tokyo Institute of Technology, Yokohama 226-8502, Japan; matsuoka.m.ab@m.titech.ac.jp*
[(3)] *Associate Professor, University of Toyama, inoguchi@sus.u-toyama.ac.jp*
[(4)] *Senior Researcher, MS&AD Inter Risk Research & Consulting, Inc., Ken.kawabe@ms-ad-hd.com*
[(5)] *Fellow, MS&AD, MS&AD Inter Risk Research & Consulting, Inc., kei.horie@ms-ad-hd.com*

Abstract

Availability of detailed damaged building information is crucial for post-seismic recovery and damage assessment after large-scale earthquakes. Currently, damaged building information is often collected by trained municipal officers and experts of earthquake engineering at the cost of great time and human resource. To overcome costly challenges, remote sensing technologies are often used for building damage mapping. The popular approaches include use of optical and SAR (Synthetic Aperture Radar) satellite imagery. In addition, boosted by surging computational power and unprecedented progression of artificial intelligence based technologies, machine learning as well as deep learning methods for earthquake damage mapping are quickly introduced and showed their promising results.

However, the damage grades of the affected buildings are evaluated by not only appearance of buildings but also their inclinations in Japan. In other words, fine-grained geometrical information is needed to assess the building damages. Satellite imagery such as optical and SAR are merely able to provide bird-eye-view images that contain less geometrical information of the buildings. On the other hand, airborne LiDAR (Light Detection and Ranging) technology is able to acquire precise 3-dimensional information in the form of point cloud from disaster-affected area immediately, which greatly widens the possibility of rapid and detailed information acquisition for emergency response and post-event recovery. Existing approaches adopting LiDAR data tend to convert 3D point cloud into grid-based DSM (Digital Surface Model), and thus such a conversion loses geometrical information through sampling from irregularly distributed points to regular grid, which is crucial to fine-grained building damage recognition. Besides, suitability of their approaches are limited to apply on such geometry-based damage evaluation framework.

Another challenges that hinder the application of powerful machine / deep learning based methods on building damage mapping are the lack of precisely annotated dataset. In spite of their surprising successes on various computer vision related tasks, machine / deep learning algorithms are usually provided with large-scale dataset in order to learn the meaningful pattern from data. Even though such large-scale dataset for building damage mapping exists for satellite imagery, there is no 3D point cloud dataset for the task.

Therefore, in order to stimulate more suitable application of machine / deep learning on building damage mapping, this study created post-event LiDAR point cloud dataset by manually assign each point of buildings a damage grade label. To the best of our knowledge, this is the first trial of creating large-scale 3D point cloud dataset for damage mapping purpose. In addition, this paper presents a quantitative evaluation of standard 3D-based machine / deep learning methods on point cloud dataset for baseline testing. The point cloud data was acquired by airborne LiDAR on 23 April 2016 following the mainshock activity of the 2016 Kumamoto Earthquake. The resulting annotated dataset contains common urban classes such as ground and tree while it includes damaged building classes defined according to their damage grades as well. We firstly describe the annotation method for creating dataset and basic statistics to demonstrate the characteristics of created dataset. We then provide baseline experiments and analysis under different classification settings. We believe that created dataset and insights from baseline experiments are valuable for future research.

Keywords: Damage Mapping; Earthquake; Machine Learning; Point Cloud;

1. Introduction

Earthquakes are one of the most catastrophic category of natural disasters that bring great damages to mankind. Taking 2016 Kumamoto Earthquake in Japan as an example, it caused more than 3000 casualties including 273 people were killed [1]. It has also caused tremendous damages to buildings in the affected area, which strongly slowed down the recovery process and imposed huge financial burden to the affected citizens as well as involved municipals. Although it is difficult to predict and avoid earthquakes, it is possible to react to it effectively in order to assess the damage and quickly recover from it. For its ability to capture data from a distant sensor platform, remote sensing technologies are frequently used for monitoring and evaluating natural disasters. For example, Matsuoka and Yamazaki used SAR (Synthetic Aperture Radar) intensity images to assess the building damages caused by 1995 Hyogoken-Nanbu earthquake [2]. Tong et al. examined the use of pre- and post-event high-resolution optical imagery to detect damages due to the May 2008 Wenchuan earthquake [3]. Additionally, Moya et al. used grid data converted from LiDAR (Light Detection And Ranging) point cloud to analyzed the building damage due to the 2016 Kumamoto earthquake [4].

Recently, increasing use of machine / deep learning technologies in computer vision domain has also made profound impact on image-based natural disaster-induced damage assessment. For instance, given high-resolution SAR imagery, Wieland et al. formulated building damage detection as a change detection using SVM (Support Vector Machines) to classify damaged buildings into different damage levels [5]. Furthermore, powered by the surprising success of CNN (Convolutional Neural Network), Xu et al. managed to show the generalization ability of several deep learning based architecture across different events [6].

However, Unified Loss Evaluation Method (ULEM) [7] defined by Cabinet Office of Japan for earthquake damage grade assessment calculates the damage score according to visual appearance including building parts as well as inclinations. The satellite imagery based approaches are merely able to provide bird-eye-view images that contains less geometrical information of buildings, e.g., height and inclinations. Therefore, their suitability is limited for damage grade assessment. On the other hand, LiDAR point cloud data can capture precise geometry of damaged buildings, and thus it has more potential to detect and recognize earthquake induced damages. Unfortunately, though there is existing large-scale satellite imagery dataset for damage recognition [7], the 3D point cloud dataset with accurate annotation for damage mapping does not exist.

Therefore, to stimulate the use of suitable 3D machine / deep learning approach for 3D damage mapping, this study aims at making following contributions:

- Create first post-event 3D point cloud dataset for 3D damage mapping (preliminary)
- Baseline test using the created dataset

We experimentally created point cloud dataset for exploring the possibility of 3D building damage mapping. To the best of our knowledge, this is the first point cloud dataset created for 3D damage mapping. The damage grades to which each point data belongs were annotated manually according to the result of field survey conducted after mainshock event of 2016 Kumamoto earthquake [9]. In addition to the defined damage grade in the field survey, we assigned “story-collapsed” damage class in order to provide more insights into the nature of building damage according to the results provided by the work of Kawabe et al. [10]. For baseline test purpose, traditional as well as cutting-edge machine / deep learning algorithms were adopted for several differently defined damage classification baseline experiments. Additionally, we repeated same classification procedures using the result of second stage field survey for comparing the effect of different ground truth. We believe that created dataset with its annotation method and baseline experiments will provide valuable insights for future earthquake damage mapping.

2. Data source

2.1 Post-event LiDAR dataset

The post-event LiDAR dataset [11] is acquired on 23 April 2016 following the mainshock activity of Kumamoto earthquake. This LiDAR point cloud dataset has the point density of 4.47 pts/m^2 covering the central part of Kumamoto Prefecture including Mashiki Town where the severest building damage occurred. In this study, the annotation regions were experimentally selected from the central area of Mashiki Town.

2.2 Damage survey data

After the event, local governments in Kumamoto Prefecture have carried out the filed survey in order to assess the building damages and issue the disaster-victim certificate to affected citizens by which they were able to receive various aids from local governments [12]. In Mashiki Town, this field survey was conducted in two stages. The first stage investigation assessed the damage by viewing the appearance, measuring the inclination and subsequently damage degrees of buildings were calculated by weighted summation of damage ratio from roof, walls and base of buildings according to ULEM. Note that in the first stage investigation, all the procedure was conducted outside the building. On the other hand, the second stage investigations were conducted in the same manner except for the fact that the weighted summation of damage degrees were calculated from both viewing the damage status from inside and outside the building, and thus more building parts such as pillars and ceilings were considered. The second investigations were implemented only when the victims were not convinced by the result of first stage investigation.

The recorded damage degrees are “no” damage, “minor” damage, “moderate –” damage, “moderate +” damage and “major” damage, respectively. All the investigation results were digitized along with the GPS locations indicating the approximate location of surveyed buildings. In addition to this classification of damage degrees defined by the Cabinet Office of Japan, Kawabe et al. has created “story-collapsed” building dataset, which originally belongs to “major” damage category, by examining external photographs of damaged buildings based on the field survey results provided by Mashiki Town government. In this paper, these two dataset are used jointly as the ground truth of damage degrees for creating damaged building dataset. Specifically, “story-collapsed” buildings in “major” class are re-annotated as “story-collapsed” class. Fig.1 shows the overview of study area with spatial distribution of annotated damaged buildings.

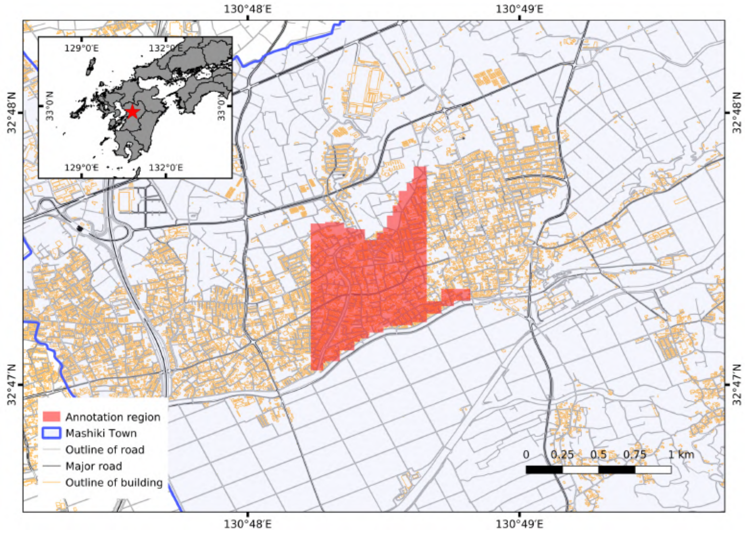

Fig. 1 – Study area and selected region for annotation. The “Damage distribution” shows the overview of spatial distribution of damaged buildings in annotated LiDAR dataset

3. Annotation detail

In this section, the detail of annotation as well as challenges encountered during annotation process are presented.

3.1 Annotation process

Post-event LiDAR point cloud data and Damage survey data are used for creating the 3D point cloud damaged building dataset. Concretely, each point of residential buildings in LiDAR point cloud data were assigned one of the class from “no” damage, “minor” damage, “moderate –” damage, “moderate +” damage, “major” damage and “story-collapsed” damage provided by damage survey data. Firstly, the points belong to a particular building were identified according to the GPS coordinate recorded in the damage survey data. Then a corresponding damage degree was assigned to all points that belong to the building. In the meantime, non-residential buildings were also annotated in order to exclude its effect in baseline experiments. The other classes such as ground, tree and other non-ground objects were annotated as well and treated as “background” class in the baseline experiment phase.

3.2 Rules and Challenges

In practice, we found that points belong to roofs of the buildings are densely distributed while the other parts, e.g., walls, are sparsely distributed in the LiDAR data. The typical building is shown in first row of Fig.2. Furthermore, the type of buildings in the study area are mostly residential houses with some platforms extended from walls such as balcony. In such cases, reflected signals from the side of buildings are possibly contaminated by some objects such as plants. Therefore, to reduce the erroneous annotations for damaged buildings, we have only annotated roofs for those who belong to damage grades excluding “major” damage and “story-collapsed” classes. The reason for such exclusion is that for damage grades higher or equal to “major” damage usually fail to preserve the original shape due to the earthquake, and hence their roofs as well as the debris were also included in annotations when it exists. The example is shown in second row of Fig.2.

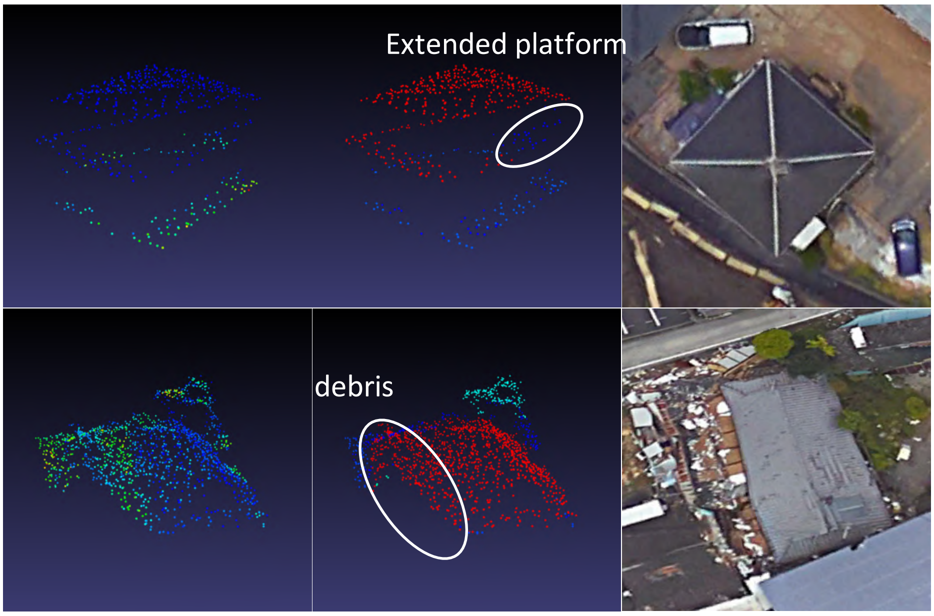

Fig. 2 – Sample annotated buildings. Left: intensity images of “minor” (top) and “story-collapsed” (bottom) building. Middle: annotation results. Red points are building. Right: aerial images of buildings.

Other challenges were to correctly identify the building points as well as debris from irregularly distributed points. We found that it was hard to discriminate the boundary points between buildings and other classes such as trees by merely relying on backscatterd amplitude information. Therefore, we also utilized Google Earth historical imagery on 30 April 2016 to provide additional color information for assisting us to better discriminating objects. Furthermore, some of the GPS coordinate of buildings were showing the locations that quite far from the actual ones. For these cases, we used in-situ photographs taken by investigators as auxiliary information to make sure the exact correspondence of annotations and damage information.

Lastly, results of annotations contain both results from first and second stage investigations. Noted that ground truth of those buildings that were only investigated once remained same in the second stage investigation. The resulting class distribution is shown in Table 1 and oblique overview of the data is shown in Fig.3.

Table 1 – Class distribution of annotated dataset

Class	**No**	**minor**	**moderate -**	**moderate +**	**major**	**story-collapsed**	**total**
First stage ground truth with story-collapsed (points)	4,121	346,330	123,924	55,710	221,942	59,590	811,617
Second stage ground truth with story-collapsed (points)	3,275	246,269	177,585	53,561	271,337	59,590	811,617

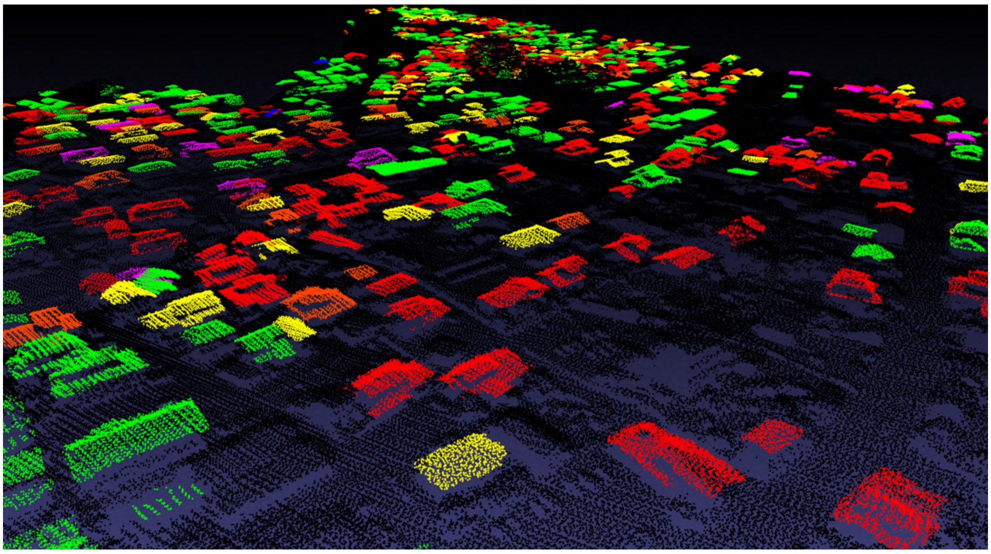

Fig. 3 – Oblique view of created dataset sample. The points are color coded by their damage grade.

4. Baseline evaluation framework

In this section, the key components of evaluation framework are explained. Firstly, the features used in classification was introduced. Subsequently, tested baseline algorithms are briefly explained. Finally, the evaluation metrics for classification in this study and implementation details are elaborated.

4.1 Feature calculation

In this paper, different types of commonly used features were used for supervised classification tasks. Most of the geometrical features were defined by following the work of Thomas et al. [13]. Besides, we defined a few additional features as follows: AGL (Above Ground Level) was computed using LAStools [14]; Height difference features were computed as the difference between the elevation value of a selected point and the lowest point within its 15m radius neighborhood; Instead of color features, which are not available, point-wise backscattered amplitude information with its mean and variance in defined neighborhood was computed; Return count information was obtained directly from LiDAR data; Horizontal angle feature that represents angle between local surface normal with horizontal plane was calculated for all points within 1m neighborhood. All the features excluding AGL, Height difference, Amplitude, Return count information and Horizontal angle were repeatedly computed for multiple definition of neighborhood to capture multi-scale features. The examples of calculated features are shown below in Fig.4. In this paper, the scales were experimentally defined as 2m, 4m and 8m, respectively. Therefore, 66 features were used for classification in total.

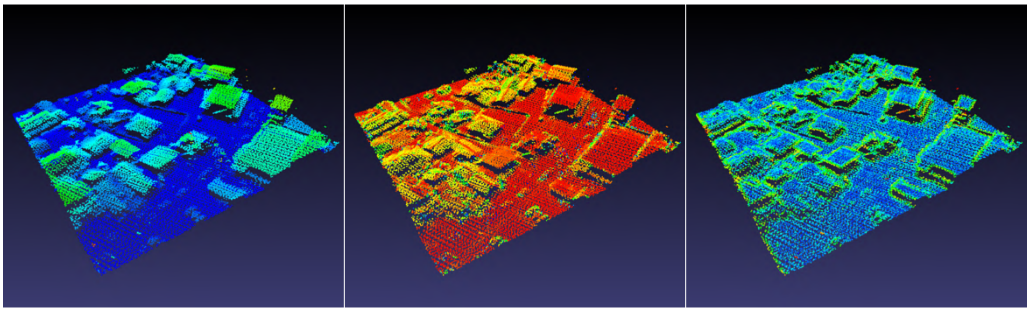

Fig. 4 – Example of calculated features: Left: AGL; Middle: Horizontal angle; Right: Linearity

4.2 Algorithms

In this study, several machine / deep learning algorithms are employed for classifications.

4.2.1 Random Forests

Random Forest [15] is a classifier that consists of multiple Decision Trees. Decision tree is a type of methods that recursively splits the feature space into a set of rectangles and then fits a value (in the case of regression) or a majority vote (in the case of classification). Individual tree is a conceptually simple yet powerful model that can approximate highly non-linear relationship of data by choosing the input features and split-point (feature value). In the case of classification, Random Forests takes majority vote from all individual trees to generate final vote. Improving the performance of a machine learning algorithm is essentially a trade-off between model variance reduction and bias reduction. Novelty of Random Forests is to improve the variance reduction by reducing the correlation between individual trees in tree growing process. Specifically, this de-correlation is achieved by random feature sub-sample when deciding a split-point. For further theoretical explanation of the algorithm, please refer to [15].

4.2.2 LightGBM

LightGBM [16] is an algorithm developed based on the idea of boosting. Similar to Random Forests, the committee of classifiers are involved in boosting. However, instead of getting majority vote as classification results, boosting sequentially applies classifiers to the modified version of data. Each data point in the dataset fit by a classifier is individually weighted, and these weights are updated during the training process. The main idea of boosting is to sequentially apply classifiers to correct the errors made by previous classifiers and thereby produce overall good model at last by weighted majority vote. Based on fundamental boosting principle, LightGBM additionally implements Gradient-based One-Side Sampling and Exclusive Feature Bundling to improve efficiency and scalability of the model. In this study, we adopted LightGBM with Gradient Boosting Decision Trees for classification tasks.

4.2.3 PointNet

PointNet [17] is a recently proposed deep neural network based algorithms that directly take raw 3D point cloud as input. PointNet is an innovative deep neural network that firstly consumes raw point cloud and obtain point-wise feature by shared multi-layer perceptrons followed by max-pooling to aggregate individual features to generate global features. Then the classification is done by stacking local and global features together, and hence both individual point as well as its neighborhood information is considered. This simple and innovative idea achieved state-of-the-art performance at the time of publication and it is still a competitive algorithm for various tasks.

4.2.4 DSGCN

Being different from PointNet, DSGCN (Dynamic-Scale Graph Convolutional Network) proposed by Xiu et al. is a deep neural network that take point cloud in the form of dynamically changing k-neighbor graph in order to model the complex local neighborhood structures [18]. The k-neighbor graphs are dilated or shrunk randomly at each sampling iteration to capture scale-invariant features in a computationally efficient manner. Furthermore, different scales of the k-neighbor graphs are combined to generate multi-scale features for final predictions. The experimental results showed that DSGCN is accurate while being robust to data corruptions.

4.3 Evaluation metrics

Results of classification are typically evaluated by TP (true Positive), FP (False Positive), TN (True Negative) and FN (False Negative) statistics that derive from confusion matrix. Since the dataset is highly imbalanced, the overall performances of the classifiers are measured by $fscore$, which is the harmonic mean of $precision$ and $recall$ metrics where $precision = TP/(TP + FP)$, $recall = TP/(TP + FN)$ and $fscore = 2\, precision \times recall\, /(precision + recall)$, respectively.

4.4 Implementation details

The whole annotated region was divided into 100m × 100m tiles. Subsequently, 80% of the tiles were assigned as training data while remaining tiles were assigned as validation. The distribution process was completed through two stages: Firstly, we have randomly distributed tiles until at least 1 sample of each class exists in both dataset; Next, remaining tiles were again randomly assigned until the distribution ratio was achieved. This process was repeated 5 times for 5-fold cross validation. For the evaluation, all points were predicted. Noted that through all processes, non-residential building points and non-labelled building points (due to lack of ground truth) were excluded.

For Random Forests and LightGBM, the minimum sample population among involved classes are assigned as sample number. The rest of the classes were randomly under-sampled. For PointNet and DSGCN, all sampling process were done on-the-fly. We adopted cross entropy as loss function with weights calculated using Eq. (1). The training was terminated after 200 epochs with batch size 32.

$$weight(C) = \ln(1.02 + \frac{sample\ number\ of\ class\ C\ in\ the\ dataset}{total\ number\ of\ samples\ in\ the\ dataset}) \quad (1)$$

5. Result and discussion

In this section, experimental results with 5-fold cross validation are illustrated and explained. In total, four types of experiments were conducted: "major and story-collapsed" and "other damage" classification, "story-collapsed" and "other damage" classification, separated damage classification and comparison of classification results using first and second stage investigation results. Note that "no" damage buildings were combined with "minor" damage buildings because they have too small number of samples.

5.1 "background", "major and story-collapsed" and "other damage" classification

It is of paramount importance to recognize higher grade building damages to rescue people in danger as soon as possible. According to Fig.5, the "background" and "other damage" classes are well separated while "major and story-collapsed" class scored lower than them. The "background" class is well separated from other classes because majority of them are simple objects such as ground and tree. The main misclassifications were introduced mainly "major and story-collapsed" class. "major" class contains not only the "crashed" buildings but also the buildings with greater inclination or having damage at its base but without visible exterior deformation. For the former case, the characteristics of building is closer to "story-collapsed" class while it is closer to "other damage" class for the latter case. On the other hand, major ambiguity between "background" and "major and story-collapsed" is debris. The classifiers were able to detect debris but increased false alarms such as low trees near the houses and ground with large slope.

Compared to Random Forests and LightGBM, deep learning based models have lower overall performance and increased variance for all classes. This result may due to the small sample population as deep learning usually needs more samples than traditional machine learning methods. Another presumable reason is imbalanced distribution of training data. Unlike Random Forests and LightGBM, which received same number of training samples for each class, the training samples were drawn randomly in every sampling iteration. Therefore, the sampled training data should approximately follow original distribution, which are extremely imbalanced. Under such a condition, DSGCN outperformed PointNet in every metrics. The increase of performance probably attributes to the exploitation of local structures by k-neighbor graph, which can model the interactions among neighboring points better than PointNet.

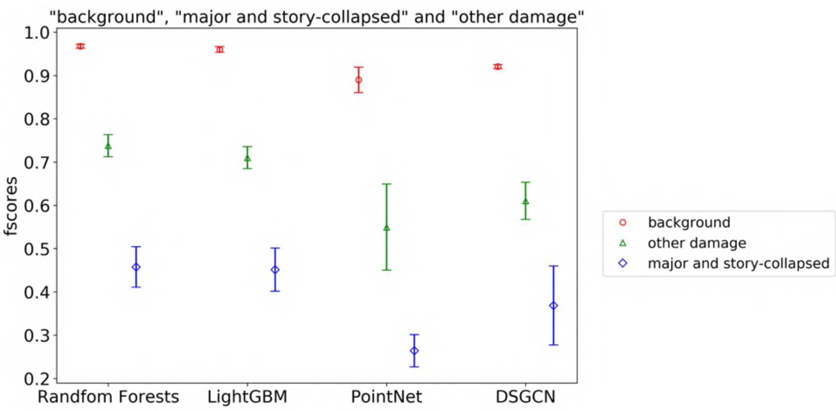

Fig. 5 – Classification results of "background", "major and story-collapsed" and "other damage"

5.2 "background", "story-collapsed" and "other damage" classification

To justify the arguments made in the former experiments, in this experiments we combined "major damage" into "other damage" class. As a result, Fig.6 illustrates that misclassification of "other damage" decreased and thus the performance was vastly increased by approximately 0.2 in terms of fscore. This result is consistent with our initial arguments. However, the ambiguity between "crashed" "major" class and "story-collapsed" class still exists so as the ground and debris inseparability. The relative high variance of "story-collapsed" class is possibly due to the reduction of available training samples since "major" class was moved to "other damage" class. This is most obvious for deep learning based models, which scored poorly because of reduced samples.

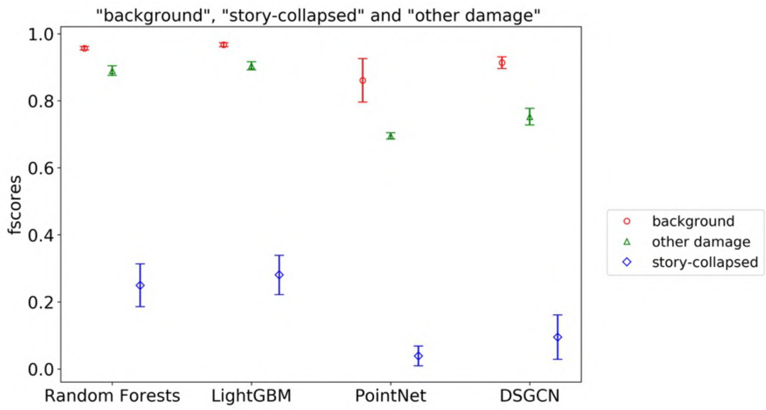

Fig. 6 – Classification results of "background", "story-collapsed" and "other damage"

5.3 Separated damage classification

To investigate separability of each damaged building class, we have implemented six class classification experiments. The overall results shown in Fig.7 were consistent with our intuition that extreme cases such as "major" and "story-collapsed" are easier to be identified, while intermediate classes are difficult to be correctly identified. The misclassification among intermediate classes were proportional to the sample numbers, which indicated that the classes are almost inseparable given used hand-crafted features. Despite deep learning based methods did not rely on the hand-crafted features, they suffered from insufficient sample populations, and hence their performances were not stable. Furthermore, it is most obvious in this classification result that multiple damage grade predictions exist in one building, which is impossible in reality.

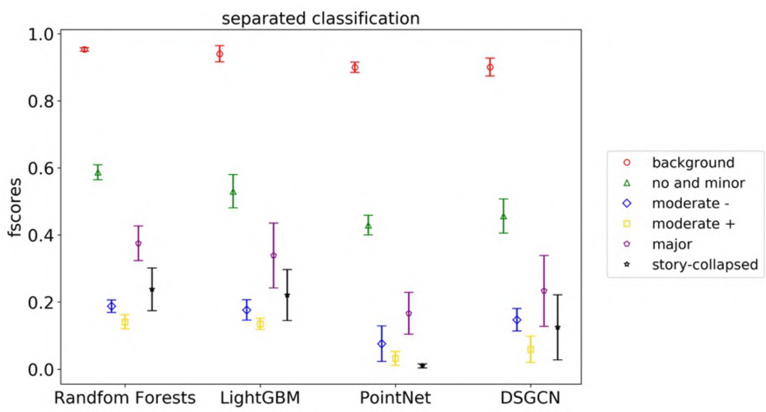

Fig. 7 – Results of separated damage classification

5.4 Comparison of first stage and second stage investigation

In this experiments, we investigated the effect of using different ground truth using only LightGBM for experimental purpose. Fig.8 shows that the first and last classification result was showing performance changes that positively correlated to the number of shift of damage grade due to second investigation results presented in Table 1. This indicates that classifier's performance is highly dependent on the number of samples, which means either the number of samples are insufficient or the current features set are ineffective for damage mapping. For the results in the middle column, the classification results were almost identical because all the classes involved were not changed before and after second stage investigation.

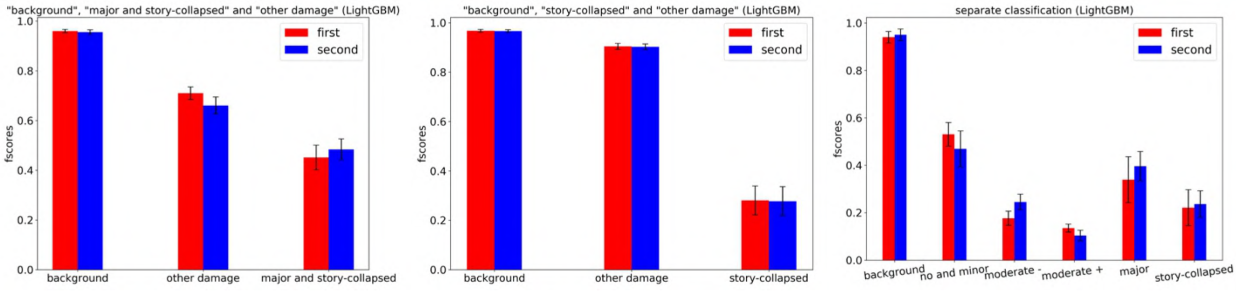

Fig. 8 – Comparison of classification results using first and second stage investigation ground truth (LightGBM)

6. Conclusion

In this study, the first 3D post-event LiDAR dataset was created for 3D building damage mapping. The detailed annotation method and related challenges were presented. Subsequently, experiments using different classification settings are conducted for baseline tests. The results revealed that it is still challenging to obtain good result in terms of used performance metrics given commonly used 3D hand-crafted features or deep learning algorithms. We believe that our attempt to create dataset and insight from several baseline experiments under different classification settings are valuable for future research on 3D based damage mapping. Future works include continue generating more annotations as well as developing point cloud based algorithms / features for 3D damage mapping.

7. Acknowledgements

This research was supported in a part by "the Tokyo Metropolitan Resilience Project" of the Ministry of Education, Culture, Sports, Science and Technology (MEXT) of Japanese Government and the National Research Institute for Earth Science and Disaster Resilience (NIED). This work is based on data services provided by the OpenTopography Facility with support from the National Science Foundation under NSF Award Numbers 1833703, 1833643, and 1833632. Digitized building and road data is provided by Geospatial Information Authority under the Ministry of Land, Infrastructure, Transport and Tourism of Japan. Google Inc. provided the historical imagery of the annotated on Google Earth.

8. References

[1] Cabinet Office of Japan. (2019). On the damage situation of 2016 Kumamoto regional earthquake in Kumamoto Prefecture, http://www.bousai.go.jp/updates/h280414jishin/pdf/h280414jishin_55.pdf (in Japanese).

[2] Matsuoka, M., & Yamazaki, F. (2004). Use of satellite SAR intensity imagery for detecting building areas damaged due to earthquakes. *Earthquake Spectra*, ***20*** (3), 975-994.

[3] Tong, X., Hong, Z., Liu, S., Zhang, X., Xie, H., Li, Z., … & B, Feng. (2012). Building-damage detection using pre- and post-seismic high-resolution satellite stereo imagery: A case study of the May 2008 Wenchuan earthquake. *ISPRS Journal of Photogrammetry and Remote Sensing*, **68**, 13-27.

[4] Moya, L., Yamazaki, F., Liu, W., & Yamada, M. (2018). Detection of collapsed buildings from lidar data due to the 2016 Kumamoto earthquake in Japan. *Natural Hazards and Earth System Sciences*, ***18***(1), 65.

[5] Wieland, M., Liu, W., & Yamazaki, F. (2016). Learning change from synthetic aperture radar images: Performance evaluation of a support vector machine to detect earthquake and tsunami-induced changes. *Remote Sensing*, ***8*** (10), 792.

[6] Xu, J. Z., Lu, W., Li, Z., Khaitan, P., & Zaytseva, V. (2019). Building Damage Detection in Satellite Imagery Using Convolutional Neural Networks. arXiv preprint arXiv:1910.06444.

[7] Cabinet Office of Japan. (2013). Operational guideline for damage assessment of residential buildings in disasters, http://www.bousai.go.jp/taisaku/pdf/h3003shishin_all.pdf (in Japanese).

[8] Gupta, R., Hosfelt, R., Sajeev, S., Patel, N., Goodman, B., Doshi, J., ... & Gaston, M. (2019). xBD: A Dataset for Assessing Building Damage from Satellite Imagery. arXiv preprint arXiv:1911.09296.

[9] Yamazaki, F., Suto, T., Liu, W., Matsuoka, M., Horie, K., Kawabe, K., ... & Inoguchi, M. (2019). Development of fragility curves of Japanese buildings based on the 2016 Kumamoto earthquake. *2019 Pacific Conference on Earthquake Engineering*, Auckland, New Zealand.

[10] Kawabe, K., Horie, K., Inoguchi, M., Matsuoka, M., Torisawa, K., Liu, W., & Yamazaki, F. (2020). Extraction of Extraction of Story-collapsed Buildings by the 2016 Kumamoto Earthquake Using Deep Learning. *Proceedings of 17th World Conference on Earthquake Engineering*, Sendai, Japan (in press).

[11] Chiba, T. (2018). Post-Kumamoto earthquake (2016) rupture lidar scan airborne lidar survey. Air Asia Survey Co., Ltd, distributed by OpenTopography. Retrieved from https://doi.org/10.5069/G9SX6B9T

[12] Mashiki Town Government. (2017). Review report on the response to the 2016 Kumamoto earthquake, https://www.town.mashiki.lg.jp/bousai/kiji0032410/3_2410_1633_up_j7cvpcog.pdf (in Japanese).

[13] Thomas, H., Goulette, F., Deschaud, J. E., & Marcotegui, B. (2018). Semantic classification of 3D point clouds with multiscale spherical neighborhoods. *2018 International Conference on 3D Vision (3DV)*, Verona, Italy.

[14] Martin Isenburg. (2019). LAStools - efficient tools for LiDAR processing. https://rapidlasso.com/lastools/

[15] Breiman, L. (2001). Random forests. *Machine learning*, **45** (1), 5-32.

[16] Ke, G., Meng, Q., Finley, T., Wang, T., Chen, W., Ma, W., ... & Liu, T. Y. (2017). Lightgbm: A highly efficient gradient boosting decision tree. *Advances in neural information processing systems*, Long Beach, U.S.

[17] Qi, C. R., Su, H., Mo, K., & Guibas, L. J. (2017). Pointnet: Deep learning on point sets for 3d classification and segmentation. *Proceedings of IEEE conference on computer vision and pattern recognition*, Honolulu, U.S.

[18] Xiu, H., Shinohara, T., & Matsuoka, M. (2019). Dynamic-Scale Graph Convolutional Network for Semantic Segmentation of 3D Point Cloud. *2019 IEEE International Symposium on Multimedia (ISM)*,San Diego, U.S.

